R. Verzicco*, J.B. Flór +, G.J.F. van Heijst + and P. Orlandi*

Interactions of Dipoles with Cylinders: Experiments and Numerical Simulations

Abstract

Flow visualizations and numerical simulations of the centred collision between a dipole and a circular cylinder have shown that the main feature is the formation of oppositely signed vorticity at the cylinder wall. The thin layer of wall vorticity rolls-up in two compact patches, which couple with the primary lobes and, by self-induced motion, move away from the cylinder along curved trajectories. The diameter of the cylinder (D_C) plays an important role in the dynamics of the collision. As D_C decreases the wall vorticity increases but, since a larger dissipation is a fundamental topic which also occurs in a number of practical situations, the secondary lobe becomes less pronounced. Measurements of the vorticity distribution before and after the collision have shown that the primary lobes preserve their original relationship $\omega = f(\psi)$ and that the secondary vorticity tends to organize into structures with a similar $\omega = f(\psi)$. The differences between advection of vorticity and of passive markers have been also analysed.

Introduction

The interaction of vortices with (solid) boundaries is a fundamental fluid dynamic topic which also occurs in a number of practical situations The interaction with the ground of the trailing vortices of an airplane during take-off, or the free surface signature by the trailing vortices of submarines are two examples of the wide range of phenomena in which these flows are involved. The case of a pair of rectilinear vortices impinging on a solid flat wall has been investigated numerically and experimentally by a number of authors (e.g. van Heijst & Flór (1989), Orlandi (1990)) and the generation of secondary vorticity at the wall was found to play a fundamental role in the interaction process.

For the interaction of a dipole with a circular cylinder, the curvature of the body adds the radius as a new parameter that makes the flow more complex. A recent numerical study by Orlandi (1993) considers the interaction for no-slip and free-slip boundary conditions. In the ideal latter case, after the collision, the dipole conserves its original shape and ω-ψ scatter plots confirm that a linear

relationship is attained again. On the other hand with the no-slip condition the secondary vorticity, interacting with the primary vortex, forms two dipolar structures that move along circular trajectories. Even in this case scatter plots present a clear tendency to attain the linear relationship eventually.

The simulations by Orlandi (1993) were limited to interactions with very small cylinders since for comparison only the experiments by Homa *et al.* (1988) were available. The present study describes laboratory and computer experiments in a large range of cylinder radii. The main goal is the comprehension of the physics of the interaction process, in particular, with respect to the effect of the diameter of the cylinder. The results indicate that the smaller the diameter of the cylinder the higher is the peak vorticity at the wall. These high peak values produce large vorticity gradients and a large dissipation. As a final result the secondary lobes have a reduced intensity.

Scatter-plots between vorticity and streamfunction have been finally analysed to investigate the distribution of the vorticity inside primary and secondary vortices. Experimental results have partially confirmed those obtained by Orlandi (1992): both vortices attain the same relationship but while in the numerical simulation it is linear, in the experiments the function $\omega = f(\psi)$ has a sinh-like shape.

Numerical method

The numerical code is the same as described by Orlandi (1993), and is here summarized briefly. Although the model has the possibility to solve the 2D Navier-Stokes equations in terms of ω and ψ in general curvilinear coordinates, it is simplified by introducing a polar coordinate system with a clustering of computational points near the cylinder. Non-uniform coordinates are mandatory to accurately describe the generation and the diffusion of wall vorticity that is the leading process of the flow. For the same reason the vorticity at the cylinder wall has been obtained by differencing the vorticity definition in the radial direction. In this way the vorticity at the wall is connected with the vorticity inside the field. The external boundary was located at 4 dipole radii where the condition $\omega = 0$ was imposed.

A finite difference scheme second order-accurate in space and in time has been used to solve the equations. The nonlinear terms have been discretized by the Arakawa (1966) scheme that, in the inviscid limit, conserves energy and enstrophy. This conservation property ensures not only the stability of the calculation but also the correct energy transfer.

The advancement in time has been obtained by a third-order Runge-Kutta scheme which calculates the nonlinear terms explicitly and the viscous terms implicitly. The large stability limit ($CFL \leqslant \sqrt{3}$) allows a large Δt and a consequent CPU saving.

Experimental set-up

The experimental set-up was the same as that of van Heijst & Flór (1989) and only the main features are described. The experiments were carried out in a plexiglass tank $90 \times 115 \times 30$ cm, with a working depth of 21 cm, filled with a linearly-stratified salt solution. The vertical variation in density was obtained by using a two-tank system. In the experiments described here the final density profile was linear with the corresponding buoyancy frequency $N \simeq 1.88$ rad s^{-1}.

The dipole generator consisted of a remote controlled injection mechanism which injected the fluid horizontally, at the level of its equilibrium density ρ_S, through a circular orifice submerged in the tank. The fluid was visualized by the thymol-blue pH-indicator. After the collapse of the turbulent region and the subsequent emergence of the dipolar structure a thin-walled plexiglass cylinder of diameter D_C was placed in the tank to realize a centred collision between the dipole and the cylinder. The positioning of the cylinder was done most carefully in order to avoid the generation of internal waves that would disturb the motion of the dipole. The evolving flow was then recorded photographically at several times by a camera fixed over the centre of the tank.

In order to get quantitative information about the flow evolution a second set of experiments was carried out by adding polystyrene particles of uniform density and injecting the fluid at the level of these particles. Streak photography and digital image analysis enable to reconstruct the velocity field to determine the associated distributions of the vorticity and the stream function.

Results

Experiments

When the fluid is pushed out of the orifice it forms a 3D turbulent jet ($Re \sim O(10^3)$) that, being discharged in a stratified fluid, collapses within a time of the order of one eddy turnover-time, resulting in a 2D structure at the level of its equilibrium density (van Heijst & Flór (1989), Voropayev et al. (1991)). The resulting structure is a large-scale dipole, of diameter D_D, whose relationship between ω and ψ is nonlinear, possibly of a sinh-like shape (Flór & van Heijst (1994)). When the formation process is completed it is argued, from flow visualizations, that most of the initial vorticity is concentrated in the dipole and only very weak patches are left behind in the wake. The dipole moves along a straight trajectory with a constant velocity and, apart from viscous diffusion, the structure of the dipole does not change in time. The cylinder was placed after the formation of the dipole, when the direction of translation was evident.

When the dipole is close to the cylinder a thin layer of oppositely signed vorticity is generated at the wall. This vorticity diffuses in the field and is entrained by the two dipole halves, which advect it far from the cylinder. As a result, layers of vorticity are continuously peeled from the surface and this process continues
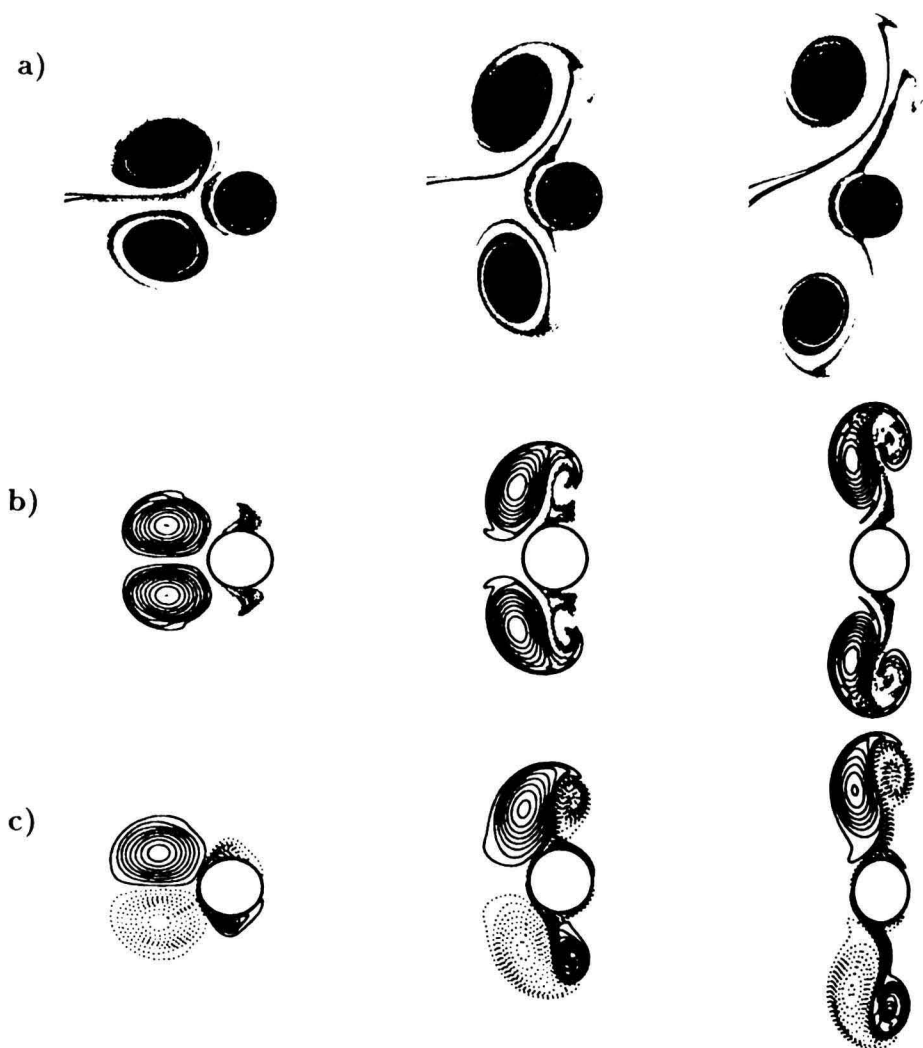
Fig. 1. Time evolution of the centred collision between a dipole and a circular cylinder, $D_D = 2D_C$, $Re = 500$. (a) Experimental results. Numerical results: (b) passive scalars released in the dipole (solid lines) and at the cylinder surface (shaded contours), (c) vorticity contour plots (solid lines for positive values, dottet for negative values). The distortion of the circular cylinder as visible in (b, c) is a graphical artifact.

even when primary structures have moved from the body. This mechanism has been evidenced by putting some fluorescein at the surface of the cylinder (Fig. 1a).

Thin layers of vorticity are very unstable and tend to roll-up to organize themselves into compact patches. Each lobe of the primary dipole couples with those patches to form asymmetric pairs moving along a curved trajectory. This

phenomenon has been observed in all experiments for different values of D_C. In particular it was observed that as D_C decreases the vortex pairs cover a larger distance downstream the cylinder and their trajectories have a smaller radius of curvature. These results agree with the numerical simulations by Orlandi (1993) who performed simulations with $D_C = 0.03D_D$. Voropayev *et al.* (1992) also showed, by experimental visualizations, that it is possible to find a suitable D_C (with $D_C \ll D_D$) such that at the final stage of the interaction a new dipole with a reduced intensity is found beyond the cylinder. This last result has been investigated numerically in more detail.

A fundamental question concerning the dynamics of coherent structures is the relationship between the vorticity ω and the stream function ψ. On short time scales viscous effects can be neglected and the structure is stationary, in a frame co-moving with the vortex. Then the Navier-Stokes equation reduces to $J(\hat{\omega}, \hat{\psi}) = 0$ with $\hat{\omega}$ and $\hat{\psi}$ the vorticity and the stream function evaluated in the co-moving frame. Provided that the function f is integrable, any $\hat{\omega} = f(\hat{\psi})$ satisfies $J(\hat{\omega}, \hat{\psi}) = 0$, showing that a large class of solutions f are possible. In the present work the function f has been evaluated by the velocity field obtained from the digitization of the streak photographs. In Fig. 2 scatter plots of $\hat{\omega}$ and $\hat{\psi}$ are shown before (Fig. 2a) and some time after the collision (Fig. 2b). After the collision the lobe of the main structure maintains its coherence while the vorticity generated at the cylinder organizes to form the second branch in the scatter-plot which has a different slope than the original one. The comparison between Fig. 2a and 2b provides evidence that after the collision the $\hat{\omega} = f(\hat{\psi})$ relaxes towards a relationship with a uniform slope which is approximately the same slope as that of the original vortex dipole.
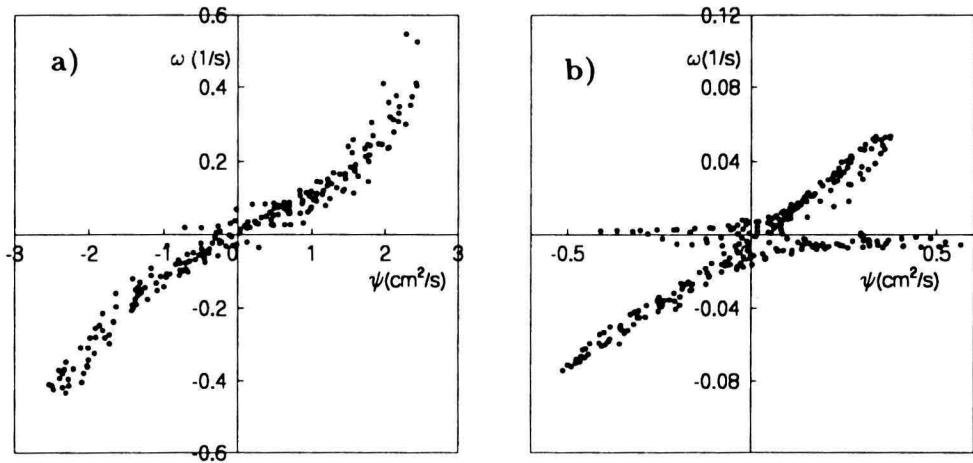

Fig. 2. Scatter plots of ω and ψ: (a) before the collision, (b) after the collision (only the upper half of the domain is considered).

Numerical Results

To simulate the initial condition of experiments with a simple model, the Lamb (1932) solution ($\omega = k^2 \psi$) has been modified with the vorticity peaks slightly displaced. The displacement of the peaks produces a shift in the positive and negative branches of the initial scatter plot resembling the sinh-like ω-ψ relationship of Fig. 2a.

Simulations with different cylinder diameters have shown that the smaller the value of D_C the larger is the wall vorticity (since $\omega \sim V_1/R$, where V_1 is the tangential velocity and $R = D_C/2$) (Fig. 3). This high vorticity is confined within thin layers and, because of the intense gradients, a large dissipation occurs. As a consequence the secondary lobes are not intense like the high wall vorticity would suggest. The trajectories of the upper main lobe are shown in Fig. 4. As expected for large D_C they do not present large curvatures, meaning that the positive and negative circulations are of the same order. In contrast, when $D_C \ll D_D$ the secondary lobe has a small circulation and tends to rotate around the primary lobe. The trajectory for $D_C = 0.01 \, D_D$ consists of a closed loop followed by a curve representing a translation of the structure beyond the cylinder. It means that for D_C below a certain value the dissipation is so strong that the secondary lobe is not intense enough to migrate with the primary. The primary dipole looses part of its vorticity and after the interaction a new weakened dipole forms beyond the cylinder.

In the present study attention is focussed on a collision with $D_C = 0.5 D_D$ and a Reynolds number of 500. The numerical results show the main features of the experimental observations and the vorticity contour plots (Fig. 1c) resemble the pictures of the evolving dye concentration (Fig. 1a).

The main difference between the experiment and the vorticity contours is the large dissipation of filaments of vorticity that survive for a shorter time than filaments of dye. This behaviour is characteristic of experiments with markers
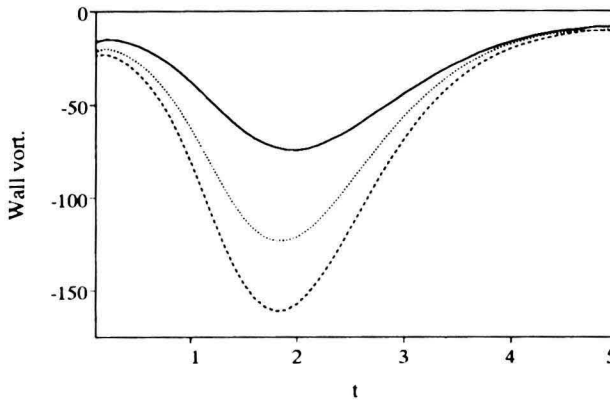

Fig. 3. Time evolution of the extremal value of the wall vorticity in the upper half plane: —— $D_C = D_D$, · · · · $D_C = 0.5 D_D$, --- $D_C = 0.25 D_D$.
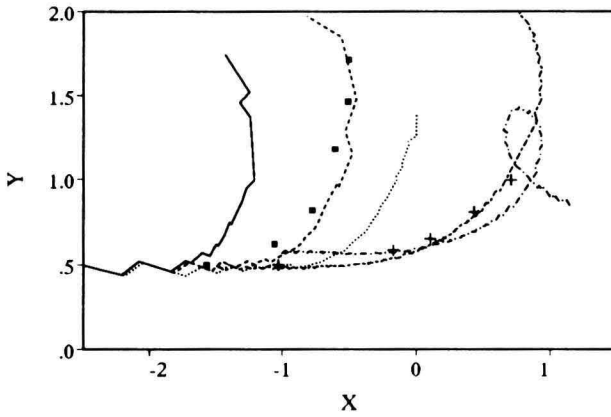
Interaction of dipoles with cylinders

Fig. 4. Trajectories of the upper primary lobe: ——— $D_C = D_D$, - - - $D_C = 0.5D_D$, $\cdots$ $D_C = 0.25D_D$, — - — $D_C = 0.03D_D$ (Orlandi (1992)), — · — $D_C = 0.01D_D$, + experiment by Homa *et al.* (1986) $D_C = 0.03D_D$, ■ present experiment at $D_C = 0.5D_D$.

and is due to the large Schmidt number which, from one side, prevents the advection of vorticity and dye to be the same but, on the other hand, allows to follow the history of the folding of layers of vorticity. For large-scale structures, where the effects of viscosity are negligible, patterns of dye and patches of vorticity behave in the same way. To evidence this behaviour the evolution of passive scalars released inside the dipole and at the cylinder surface (like the experiment of Fig. 1a) has been simulated (Fig. 1b). A Schmidt number $Sc = 10$ has been used. Although for the laboratory experiment the Schmidt number has a value $Sc \sim O(10^3)$, the numerical demonstration clearly demonstrated the effect of the reduced diffusivity. Numerical and experimental results show that, when the dipole approaches the cylinder, the shear determines the accumulation of the scalar on a small part of the cylinder surface. Subsequently the scalar is convected in the field. In contrast the vorticity is shed from a larger part of the surface, showing that the difference is due to the fact that the vorticity is continuously generated at the wall, while the passive scalar is not.

The structure of the vorticity inside the new dipoles has not been computed for this case but here we refer to results obtained by Orlandi (1993) for a similar case. The numerically determined scatter-plots show the same tendency as in the experiments: the primary lobe preserves its original relationship while the wall vorticity organizes in such a way that it attains a relationship similar to that of the primary structure.

Conclusions

Laboratory and computer experiments have been performed to investigate the dynamics of centred collisions of a dipole against a circular cylinder. In the whole range of D_C values considered, similar features have been observed, i.e. when the dipole collides with the cylinder it splits in two lobes and each one

couples with the wall vorticity to produce asymmetric dipoles moving along curved trajectories. The diameter of the cylinder has been seen to play a role in the generation of the wall vorticity and in the distance travelled, by the emerging pairs, beyond the cylinder. In particular as D_C increases the secondary lobes become more pronounced and the trajectories of the newly formed vortices become more and more orthogonal to the trajectory of the primary dipole. In contrast for small D_C ($D_C = O(10^{-2}) D_D$) the primary lobes, after moving along a closed loop, couple again beyond the cylinder. These observations are consistent with numerical simulations by Orlandi (1993).

The analysis of the distribution of the vorticity, before and after the collision, has confirmed that the primary lobes conserve their original relationship $\omega = f(\psi)$ while the secondary vorticity becomes concentrated in compact patches attaining the same f. Passive scalars and vorticity have been seen to be advected similarly in the larger structures, but quite differently in the elongated regions where the different diffusivities play an important role.

Acknowledgement

References

Arakawa, A., 1966 - Computational design for long term numerical integration of the equations of fluid motion: Two-dimensional incompressible flow. Part I. *J. Comp. Phys.* **1**, 119–143.

Flór, J.B. and G.J.F. van Heijst, 1994 - Experimental study of dipolar vortex structures in a stratified fluid. *J. Fluid Mech.* **279**, 101–134.

Homa, J., M. Lucas and D. Rockwell, 1988 - Interaction of impulsively generated vortex pairs with bodies. *J. Fluid Mech.* **197**, 571–594.

Lamb, H., 1932 - *Hydrodynamics*. Cambridge University Press.

Orlandi, P., 1990 - Vortex dipole rebound from a wall. *Phys. Fluids* **A2**, 1429–1436.

Orlandi, P., 1993 - Vortex dipoles impinging on circular cylinders. *Phys. Fluids* **A5**, 2196–2206.

van Heijst, G.J.F. and J.B. Flór, 1989 - Dipole formation and collisions in a stratified fluid. *Nature* **340**, 212–215.

Voropayev, S.I., Y.D. Afanasyef and I.A. Filippov, 1991 - Horizontal jet and vortex dipoles in a stratified fluid. *J. Fluid Mech.* **227**, 543–566.

* Università di Roma "La Sapienza"
Dipartimento di Meccanica e Aeronautica
Via Eudossiana 18, 00184 Rome, Italy

+ Fluid Dynamics Laboratory
Eindhoven University of Technology
P.O. Box 513, 5600 MB Eindhoven, The Netherlands